Application of photochromic dye to the measurement of particle movement in a fluidized bed

Application of photochromic dye to the measurement of particle movement in a fluidized bed

Takami Kai[a*], Tatsuji Kanda[a], Takeshige Takahashi[a] and Masahiro Kawaji[b]

[a] *Department of Applied Chemistry and Chemical Engineering, Kagoshima University, Kagoshima 890-0065, Japan*
[b] *Department of Chemical Engineering and Applied Chemistry, University of Toronto, Toronto, ON, Canada M5S 3E4*

---

* Corresponding author.
 Takami Kai

Department of Applied Chemistry and Chemical Engineering
Kagoshima University
1-21-40 Korimoto, Kagoshima 890-0065, Japan

Tel +81 99 285 8361; fax +81 285 8361.
E-mail address: t.kai@cen.kagoshima-u.ac.jp (T. Kai).

Abstract

A new method has been used to visualize particle movement and to observe the emulsion flow in a two-dimensional fluidized bed. The method is based on the ultraviolet light activation of particles impregnated with a photochromic dye solution. When activated, the particles changed their color to dark blue allowing their movement to be easily distinguished and tracked. This method enabled us to observe continuously the movement of bubbles and fine particles around a bubble in a fluidized catalyst bed. A detailed study of the particle movements around the bubbles showed that even when the bubble ascending velocity is large, the bubble is not accompanied by an upward emulsion flow.

Author Keywords: Fluidization; Fluidized bed; Visualization; Photochromic dye; Particle movement

---

1. Introduction

The bubble ascending velocity is one of the most important parameters for designing fluidized bed reactors. It is also an index of fluidizing quality in the fluidized catalyst bed [1]. When good fluidization is established in the fluidized catalyst bed, the mean bubble ascending velocity relative to the bed wall, ub, has been determined to be much greater than the predictions [1 and 2] of an equation given by Davidson and Harrison [3].

It is commonly supposed that the behavior of fluidized catalyst beds is similar to that of bubble columns with bulk recirculation [2 and 4]. There exists an intense circulation of liquid in the bubble column, which results from the ascending bubble-rich phase in the central region of the column and the descending phase of low bubble population in the peripheral region. Under such a condition, gas bubbles ascend with a large velocity because they are accompanied by the up-flowing liquid. The large value of ub in the fluidized catalyst bed is considered to be due to a similar mechanism. Although the particle movement around a single bubble has been well investigated [5, 6, 7, 8 and 9], the emulsion flow around the bubble ascending with a large velocity has not been sufficiently well understood.

Several methods have been utilized in the past to visualize particle movement in a two-dimensional fluidized bed. A recent review of these methods as well as many hydrodynamic aspects of gas–solid fluidization has been reported by Lim et al. [10]. The method using dyed particles has been the most popular method. In this method, colored particles of the same size, shape, density and Umf were added as tracer particles [9, 11 and 12]. Colored tracer particles and uncolored particles were packed separately to determine the drift line caused by the passage of a single bubble [8 and 13]. This method cannot be used for measurements in a freely bubbling bed. Although the particle movement can be observed by mixing colored particles in the case of coarse particles, it is impossible to detect the particle movement in fluidized catalyst beds with fine particles.

Morooka et al. [14] used a fluorescent dye for flow visualization of fine particles in a fluidized bed. They coated FCC particles with a fluorescent dye as tracer particles and determined the local percolation velocity of fines in the dense fluidized bed of coarse particles. Tayebi et al. [15] also used FCC particles impregnated with a fluorescent dye. They measured the particle movement by a multi-fiber optical probe. When an ultraviolet light illuminated the tracer particles, a visible light was emitted from them. The emitted light was weak but could be detected by a photo-multiplier. This method, however, needs an electronic device to detect the motion of the tracer particles and is unsuitable for observing the movements of particles and bubbles simultaneously.

In the present study, a flow visualization method called the photochromic dye activation technique has been applied to the observation of particle movement in a gas–solid system for the first time. The photochromic dye activation technique, originally developed by Popovich and Hummel [16 and 17], has enabled visualization of liquid flow in many previous studies of single-phase liquid and gas–liquid two-phase flows [18, 19, 20 and 21]. The method is based on the light activation of a photochromic dye material dissolved in a transparent liquid, and involves the subsequent monitoring of the position of the dye traces formed after activation. Many studies have used this technique to analyze the flow properties of organic liquids [18, 19, 20, 21, 22 and 23]. In these studies, 1′,3′,3′-trimethyl-indoline-6-nitrobenzospiropyran (TNSB) was mainly used. A few studies also reported on the use of aqueous photochromic dye solutions, for example, triaryl methane dye sulfite [24 and 25].

In applying this method to the observation of particle

movement in the present study, all the porous particles in the fluidized bed were impregnated with an aqueous solution containing a photochromic dye. Only the particles that were irradiated by an ultraviolet light changed their color for several seconds. This enabled the visualization of the particle movement in a freely bubbling fluidized bed. In addition, the particle size distribution was not influenced by the impregnation and the particle density was adjustable. One of the objectives of the present study was to expand the photochromic dye activation technique to the observation of the particle movement in gas–solid systems. The other objective was to apply this method to observe the flow of the emulsion phase around the ascending bubble that ascends with large velocities in the fluidized catalyst bed.

2. Experimental equipment and procedure

2.1. Pretreatment of particles

Porous alumina particles with an average diameter of 54 μm and a dry particle density of 870 kg m^{-3} were used in the present experiments. They are categorized to fall in Geldart's A group [26]. The shape of the particles was almost spherical. The size distribution was wide and the content of fine particles less than 44 μm was 22%. The pores of all the alumina particles were impregnated with an aqueous solution of a photochromic dye. Therefore, all the particles in the bed became the latent tracer. The particle density after impregnation increased to 1610 kg m^{-3}, and U_{mf} was 2.4 mm s^{-1}. Good fluidity was achieved even after the impregnation. The particle agglomeration due to liquid bridging was not observed, because the solution loading was controlled not to overflow from the pores.

The concentration of the dye in the solution was 0.05% by weight. The color of the particles after the impregnation was light yellow, which turned to dark blue immediately after irradiation by an ultraviolet light beam. The contrast between the activated particles and the background particles was high enough to enable video recording of a dark blue dye spot. The color of the activated dye gradually faded by the reverse reaction and the lifetime as a tracer was limited to several seconds. In addition to this fading of the color, after the activation, the size of the spot dye trace near bubbles expanded and the contrast decreased because of particle mixing in a fluidized bed. However, a high-speed video camera enabled monitoring of the movement of the spot dye trace and collection of quantitative data on the local velocity of the emulsion phase.

2.2. Fluidized bed

The experiments were performed in a two-dimensional fluidized bed of 120×10 mm cross-section and 1.5 m height. The column was constructed of transparent polymethylmethacrylate resin sheets. Since an ultraviolet beam had to pass through the front surface of the column, this side was made of a glass plate of 3.0 mm thickness. The outer wall of the opposite side was covered with a sheet of black paper in order to increase the contrast between the emulsion phase and the bubble phase. A filter paper was arranged on top of the column to prevent particles from being carried over.

Perforated plates made of polymethylmethacrylate resin were used as an air distributor at the bottom of the column. The thickness of the plate was 2 mm and each plate had 20 holes of 1 mm diameter. A filter paper with 11 μm pores was sandwiched between the two perforated plates. The particles were fluidized by humidified air at ambient temperature. The settled bed height was 0.40 m and the superficial gas velocity,

U_f, was varied from 0.025 to 0.14 m s^{-1}.

2.3. Laser and optical equipment

A top view of the optical arrangement used in this study is shown in Fig. 1. An ultraviolet light beam from a He–Cd laser at a wavelength of 325 nm was mechanically chopped to produce light pulses of 5.56 ms duration at a rate of 30 Hz. A UV-transmitting lens with a focal length of 130 mm was used to focus the beam on the inner wall of the column and to form a small circular spot dye trace in the emulsion phase. The angle of incidence was 60°.
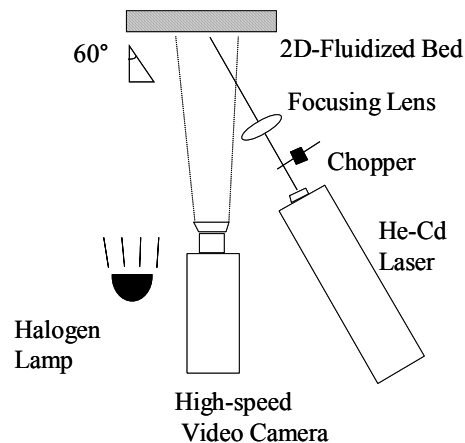

Fig. 1. Top view of optical arrangement.

To record the motion of the activated particles, a high-speed video camera system (Photron Model HSV-11B) was utilized. This system had a CCD camera with 256×256 pixel resolution, and was used to record 186 images per second with a shutter speed of 5000 s^{-1}. The bubble behavior and the motion of the emulsion phase around bubbles could be observed simultaneously by this system. The bed was illuminated with front lighting to permit distinction of the bubble phase from the emulsion phase, and to provide sufficient contrast between the activated particles and other particles.

2.4. Image analysis

The digital image data stored in the high-speed video camera system were first transferred to an 8 mm videotape using High-8 and SVHS videocassette recorders. The motion picture was transferred to a motion-picture file using a video capture board (PCAPCI-34, Canopus) installed on a personal computer (PC). The motion of each spot dye trace was then analyzed on the PC by digitizing the coordinates of the tracer particle images in a sequence of still pictures at a 5.35-ms interval. The particle velocity was calculated from the displacement of the tracer particles over the time elapsed.

3. Results and discussion

Fig. 2 shows the relationship between the superficial gas velocity and the bubble size (width) observed in the present study. As evident in this figure, the bubble size was small. This indicates that the fluidization quality was good under the experimental conditions. The average bubble holdup obtained from the heights of settled and fluidized beds, and the expansion ratio of the emulsion phase, is also shown in this

figure. Fig. 3 shows the variation of the mean bubble velocity, u_b, obtained by direct observation, with the fluidizing gas velocity. The value based on the ascending velocity of a single bubble is also plotted in Fig. 3. After the bed was fluidized at a predetermined gas velocity slightly below the minimum bubbling condition, a solenoid valve was opened for a short period of time to inject a single bubble in the bed. The values shown in Fig. 3 were calculated from the velocity of a single bubble having the same size as the average bubble size in a freely bubbling bed at each superficial gas velocity. As shown in Fig. 3, the mean bubble ascending velocity was very large in a two-dimensional bed.
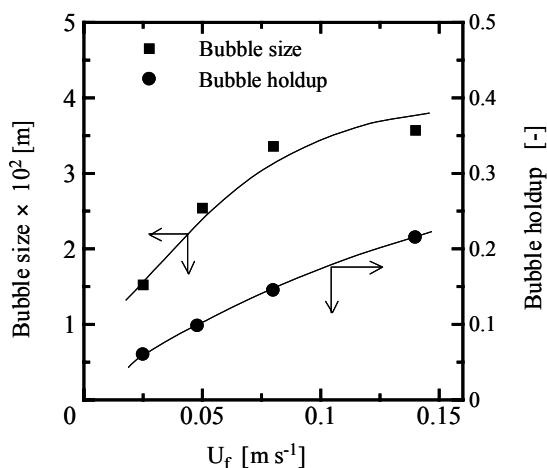

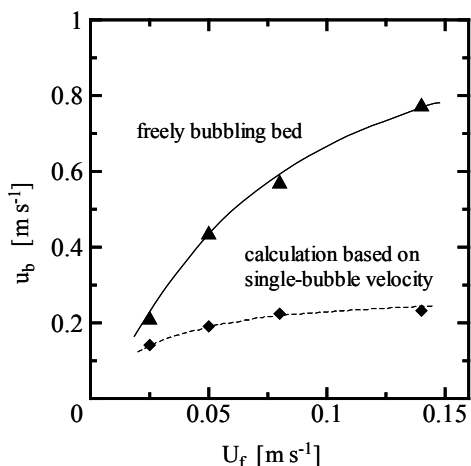Fig. 2. Effect of Uf on bubble size and bubble holdup.

Fig. 3. Ascending velocity of bubbles.

Fig. 4 shows sample photographs indicating the movement of a spot dye trace formed beside a bubble at U_f=0.05 m s^{-1}. Images are shown at a 16.0-ms interval. The dark areas in the photographs represent bubble cavities or activated particles, while the rest represents the emulsion phase. The white spots in Fig. 4(a) and (c) show the reflection of an irradiated ultraviolet beam at the time of particle activation. They indicate the focal point of the ultraviolet laser beam. The initial diameter of the spot dye trace was about 1 mm judging from a comparison of the trace diameter with the scale shown in Fig. 4(a). Although the trace movement is difficult to obtain directly from these still images, it is easily distinguishable when the motion is continuously observed from a video tape. As shown in Fig. 4, the bubble surface continuously collapsed and the particles fell down into the bubble. The bubble deformation became

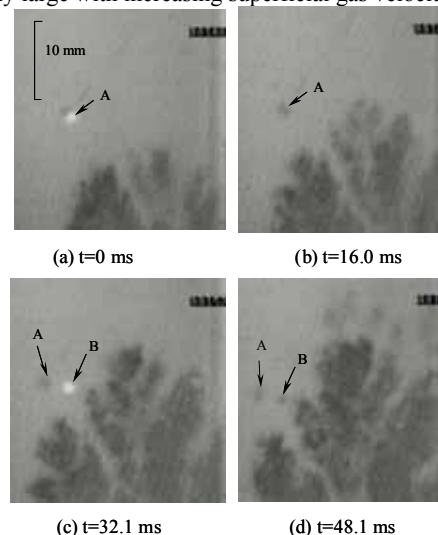remarkably large with increasing superficial gas velocity.

(a) t=0 ms (b) t=16.0 ms

(c) t=32.1 ms (d) t=48.1 ms

Fig. 4. Particle movement beside ascending bubbles.

The particle movement around a bubble at a low gas velocity (U_f=0.025 m s^{-1}) was almost similar to that reported in previous studies [8 and 9]. Fig. 5 shows the movement of the emulsion beside a bubble at U_f=0.08 m s^{-1}. The spot dye trace marked "C" moved downward constantly and spread in area as the bubble ascended. The trace traveled downward a distance of 12 mm during 48.1 ms, so the average velocity of this trace was 0.25 m s^{-1}. The average value for all the measurements was 0.2 m s^{-1}. Such movements were typical and this behavior was observed in most cases over all gas velocities. This indicated that the whole bubble was not accompanied by the emulsion flow, whereas bubbles smaller than 1 cm were fully accompanied by the up-flow of the emulsion behind a larger bubble.

(a) t=0 ms (b) t=16.0 ms
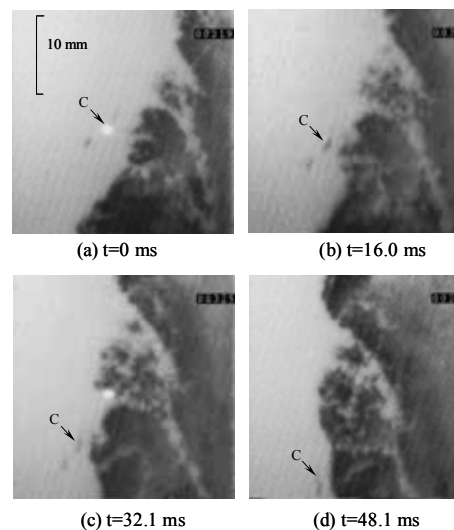
(c) t=32.1 ms (d) t=48.1 ms

Fig. 5. Particle movement beside ascending bubbles.

In the region near the lower side of a bubble, the particles moved horizontally to an area below the bubble. Some of these particles flowed upward as if following the bubble. Fig. 6 shows the upward flow of particles below rising bubbles. Each image was obtained at a 5.3-ms interval. Fig. 6(a) shows the spot dye trace formed below a bubble. The up-flow velocity of the trace marked "D" was 0.72 m s^{-1} in this case. A

considerable amount of particles was carried upward by this flow, whereas the particle velocity below the bubbles varied in the horizontal direction. Although the particle upward flow after the passage of a single bubble has been observed [8, 9 and 13], the effect was significant when the fluidizing gas was supplied continuously. Therefore, we examined the region affected by this upward flow.
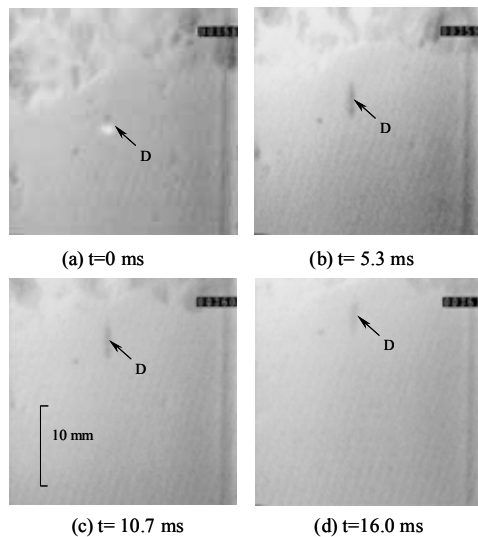

Fig. 6. Upward flow of particles below bubbles.

Fig. 7 shows the relationship between the distance from the bottom of a bubble and the ascending velocity of the particles below the bubble for different fluidizing gas velocities. The velocity of the particles just below the bubble almost agreed with u_b and decreased with increasing distance from the bottom of the bubble. When U_f=0.08 m s^{-1}, the effect of bubble passage on the particle up-flow was still evident 0.12 m below a bubble, whereas the effect was limited to within 0.03 m when the gas velocity was small. Since the bubbles were passing in succession at above U_f=0.08 m s^{-1}, the roof of each bubble was always influenced by the emulsion up-flow caused by the leading bubble. A white spot in Fig. 8(a) formed after 80 ms of the passage of a preceding bubble. The distance between the bottom of this bubble and the spot was about 45 mm. This spot dye trace followed the bubble and ascended with an average velocity of 0.4 m s^{-1}. The vertical velocity of the roof of the succeeding bubble was calculated to be 0.53 m s^{-1} and the bubble gradually caught up with the dye trace marked "E".

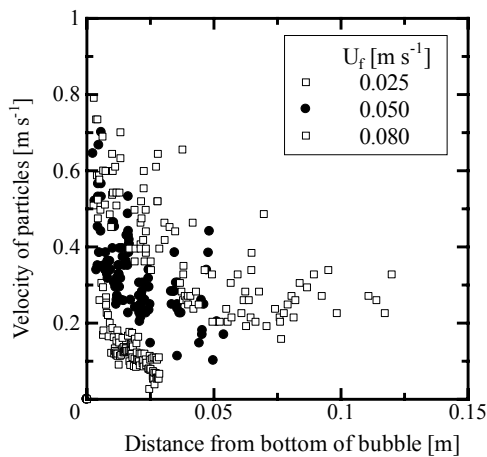Fig. 7. Relationship between distance from bubble
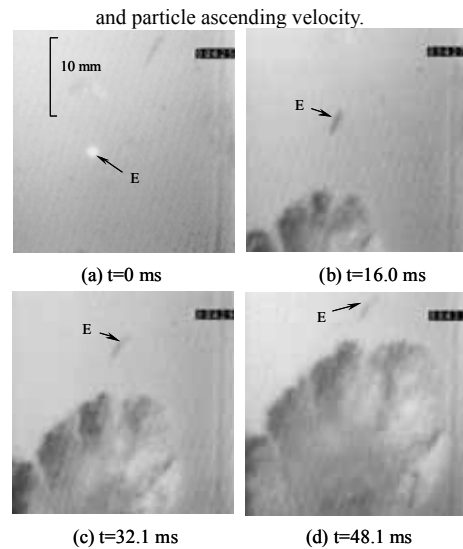
and particle ascending velocity.

Fig. 8. Movements of spot dye trace and succeeding bubble cavities.

While the roof of a bubble was affected by an ascending emulsion, the bubble suffered a large shear stress because the emulsion phase flowed downward past the side of the bubble. Since the bubbles could not keep their shape, they deformed and split due to the shear stress. Typical features of bubble flow observed in a two-dimensional bed are illustrated in a simplified manner in Fig. 9. The length of the arrows in the figure almost corresponds to the velocity of the flow relative to the wall. The upward flow of the emulsion and bubbles formed a stream that fluctuated with time. The large value of ub is considered to be due to the above feature of the flow. However, since the emulsion flows downward past the side of the bubbles in fluidized catalyst beds, the mechanism is rather different from that in bubble columns. The shear stress acting on a bubble causes the bubble to split into several smaller parts. These parts then merge with the main bubble at the bottom of the main bubble. In the bubble measurements using inserted probes, many peaks could be observed for one bubble in the fluidized catalyst bed [27]. This structure can be interpreted as a cluster of small bubbles or one bubble containing a large amount of particles.
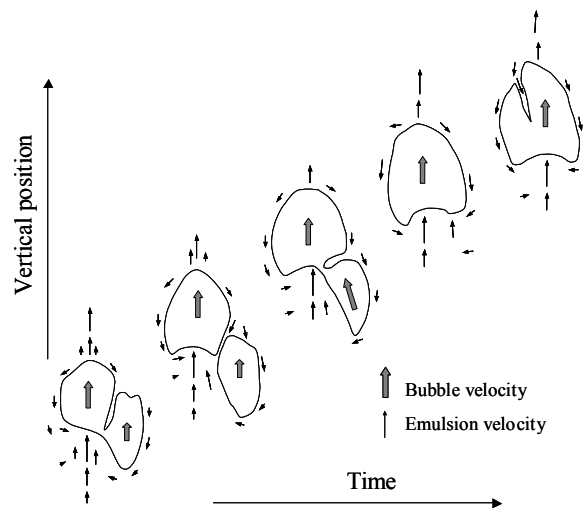

Fig. 9. Typical flow features of bubbles and emulsion.

4. Conclusions

A photochromic dye activation technique has been successfully used to visualize and analyze particle movement in a fluidized catalyst bed. This method enabled us to simultaneously measure the local velocity of particles around bubbles and observe the bubble behavior. Therefore, it became possible to analyze the bubble and emulsion flow patterns in the fluidized bed.

When the ascending bubble velocity was very large in the fluidized catalyst bed, the upward flow of the emulsion was observed below the leading bubble and above the succeeding bubble. Therefore, the roof of the ascending bubbles constantly experienced the up-flow of the emulsion and the bubbles ascended with a large velocity in this stream. On the other hand, the emulsion on the side of bubbles flowed downward and the resulting shear stress caused the deformation of bubbles and bubble splitting/coalescence.

Though the proposed method is limited to the observation of the particle movement near the bed surface and transparent wall surface, it is a useful method to continuously measure the local velocity of fine particles without disturbing the flow pattern.

List of Symbols

U_f superficial gas velocity (m s^{-1})
U_{mf} minimum fluidization velocity (m s^{-1})
u_b mean bubble ascending velocity (m s^{-1})

Acknowledgements

References

1. T. Tsutsui and T. Miyauchi Kagaku Kogaku Ronbunshu 5 (1979), pp. 40–46.
2. T. Miyauchi, S. Furusaki, S. Morooka and Y. Ikeda , Transport phenomena and reaction in fluidized catalyst beds. Adv. Chem. Eng. 11 (1980), pp. 275–448.
3. J.F. Davidson and D. Harrison , Fluidized Particles. , Cambridge Univ. Press, London (1963).
4. S. Morooka, K. Tajima and T. Miyauchi Kagaku Kogaku 35 (1971), pp. 680–686.
5. R. Jackson Trans. Inst. Chem. Eng. 41 (1963), pp. 22–28.
6. J.F. Davidson Trans. Inst. Chem. Eng. 39 (1961), pp. 230–233.
7. J.D. Murray J. Fluid Mech. 22 (1965), pp. 57–80.
8. R. Toei, R. Matsuno and Y. Nagai Kagaku Kogaku 31 (1967), pp. 457–463.
9. B. Kocatulum, E.A. Basesme, E.K. Levy and B. Kozanoglu AIChE Symp. Ser. 88 289 (1992), pp. 40–50.
10. K.S. Lim, J.X. Zhu and J.R. Grace , Hydrodynamics of gas–solid fluidization. Int. J. Multiph. Flow 21 (1995), pp. 141–193 (Suppl.) .
11. K.S. Lim, V.S. Gururajan and P.K. Agarwal Chem. Eng. Sci. 48 (1993), pp. 2251–2265.
12. A.S. Hull, Z. Chen, J.W. Fritz and P.K. Agarwal Powder Technol. 103 (1999), pp. 230–242.
13. T. Chiba and H. Kobayashi J. Chem. Eng. Jpn. 10 (1977), pp. 206–210.
14. S. Morooka, K. Kusakabe, N. Ohnish, F. Gujima and H. Matsuyama Powder Technol. 58 (1989), pp. 271–277.
15. D. Tayebi, H.F. Svendsen, A. Grislingas, T. Mejdell and K. Johannessen Chem. Eng. Sci. 54 (1999), pp. 2113–2122.
16. A.T. Popovich and R.L. Hummel , Experimental study of the viscous sublayer in turbulent pipe flow. AIChE J. 13 (1967), pp. 854–860.
17. A.T. Popovich and R.L. Hummel Chem. Eng. Sci. 22 (1967), pp. 21–25.
18. M. Kawaji, J.M. DeJesus and E.T. Tudose Nucl. Eng. Des. 175 (1997), pp. 37–48.
19. G. Karimi and M. Kawaji Chem. Eng. Sci. 53 (1998), pp. 3501–3512.
20. W. Ahmad, J.M. DeJesus and M. Kawaji Chem. Eng. Sci. 53 (1998), pp. 123–130.
21. M. Kawaji Nucl. Eng. Des. 184 (1998), pp. 379–392.
22. G. Karimi and M. Kawaji Nucl. Eng. Des. 200 (2000), pp. 95–105.
23. E. Stamatiou, P.M.Y. Chung and M. Kawaji Nucl. Technol. 134 (2001), pp. 84–96.
24. P. Douglas Chem. Eng. Technol. 14 (1991), pp. 275–287.
25. P. Douglas and R.D. Enos Chem. Eng. Technol. 15 (1992), pp. 269–277.
26. D. Geldart Powder Technol. 7 (1973), pp. 285–292.
27. T. Kai, T. Imamura and T. Takahashi Powder Technol. 83 (1995), pp. 105–110.